FOXO1 Negates the Cooperative Action of FOXL2^{C134W} and SMAD3 in CYP19 Expression in HGrC1 Cells by Sequestering SMAD3

Martina Belli,[1]* Christian Secchi,[1]* Dwayne Stupack,[1] and Shunichi Shimasaki[1]

[1]*Department of Reproductive Medicine, School of Medicine, University of California San Diego, La Jolla, California 92093*

ORCiD numbers: 0000-0003-1926-6709 (M. Belli); 0000-0001-5725-9214 (C. Secchi); 0000-0003-4396-5745 (D. Stupack); 0000-0002-2725-7039 (S. Shimasaki).

*M.B. and C.S. contributed equally to this work.

Adult granulosa cell tumor (aGCT) is a rare type of ovarian cancer characterized by estrogen excess. Interestingly, only the single somatic mutation *FOXL2^{C134W}* was found across virtually all aGCTs. We previously reported that FOXL2^{C134W} stimulates CYP19 transcription synergistically with SMAD3, leading to elevated estradiol synthesis in a human granulosa cell line (HGrC1). This finding suggested a key role for FOXL2^{C134W} in causing the typical estrogen overload in patients with aGCTs. We have now investigated the effect of FOXO1, a tumor suppressor, on *CYP19* activation by FOXL2^{C134W} in the presence of SMAD3. Intriguingly, FOXO1 antagonized the positive, synergistic effect of FOXL2^{C134W} and SMAD3 on CYP19 transcription. Similar to FOXL2^{C134W}, FOXO1 binds SMAD3 but not the proximal FOXL2^{C134W} binding site (−199 bp) of the CYP19 promoter identified in our earlier studies. The results of a competitive binding assay suggested a possible underlying mechanism in which FOXO1 sequesters SMAD3 away from FOXL2^{C134W}, thereby negating the cooperative action of FOXL2^{C134W} and SMAD3 in inducing CYP19 expression. To our knowledge, this study is the first to demonstrate the ability of FOXO1 to restore an altered CYP19 expression by FOXL2^{C134W} and SMAD3 and provides insight as to why FOXO1 deficiency promotes GCT development in mice.

Freeform/Key Words: CYP19, FOXL2, FOXO1, granulosa cell tumor, HGrC1, SMAD3

The forkhead box (FOX) family of transcription factors consists of 19 subfamilies clustered by sequence conservation, from FOXA to FOXS [1]. FOX proteins are encoded by >170 distinct genes identified in 14 species, including 50 in humans, and characterized by an evolutionarily conserved DNA-binding domain known as the FOX domain (also known as the winged-helix domain). Most FOX proteins bind to DNA as monomers [2]. They regulate a diverse range of biological and physiological activities, including developmental and homeostatic processes [3]. In the field of ovarian biology, three of the FOX family members, FOXL2, FOXO1, and FOXO3, have been extensively studied and are known to be associated with gonadal development, sterility, and tumorigenesis [4].

Studies in humans, mice, and goats demonstrated that FOXL2 is expressed in selected cell types, such as mesenchyme of developing eyelids, embryonic and adult pituitary gonadotrope

Abbreviations: aGCT, adult granulosa cell tumor; BPES, blepharophimosis/ptosis/epicanthus inversus syndrome; FBE, FOX binding element; FOX, forkhead box; GC, granulosa cell; GCT, granulosa cell tumor; HGrCl, human granulosa cell line; qRT-PCR, quantitative RT-PCR; SBE, SMAD binding element.

Received 25 July 2019
Accepted 23 August 2019
First Published Online 29 August 2019

ISSN 2472-1972
November 2019 | Vol. 3, Iss. 11
doi: 10.1210/js.2019-00279 | Journal of the Endocrine Society | 2064–2081

and thyrotroph cells, the endometrium, and fetal and adult granulosa cells (GCs) in the ovary [5–12]. Two *Foxl2* germline null mouse models developed in different laboratories displayed perinatal mortality of 50% to 95%, associated with craniofacial malformations and impaired development of the ovary and eyelid. Alternatively, the surviving female mice were infertile due to a block in follicle development at the primary stage associated with a failure of GCs to complete the squamous to cuboidal transition, suggesting that FOXL2 is essential for early folliculogenesis [11, 13]. In contrast, somatic and inducible FOXL2 knockdown experiments in adult female mice have demonstrated a second critical role, which is the maintenance of ovarian structure and function. This is supported by the fact that FOXL2 knockdown in adult female mice leads to the de-repression of *Sox9* and the ovary-to-testis sex reprogramming associated with the transdifferentiation of ovarian granulosa/theca cells into Sertoli/Leydig-like cells, the upregulation of testicular genes, the downregulation of ovarian genes, such as CYP19, and the loss of oocytes [14]. This finding suggests that the *Foxl2* gene needs to be activated throughout life to suppress male-specific gene expression in the gonad.

More than 120 germline mutations in the *FOXL2* gene have been found to be the cause for blepharophimosis/ptosis/epicanthus inversus syndrome (BPES), an autosomal-dominant disease characterized by dysplasia of the eyelids associated with (BPES type I) or without (BPES type II) premature ovarian failure [5, 15]. In contrast, a single somatic missense mutation, $FOXL2^{C134W}$, which is never observed in BPES, is found in virtually all adult GC tumors (aGCTs)—a rare, but unpredictable, type of ovarian cancer (2% to 5%). These studies included >400 tumors from patients of diverse ethnicities [16, 17]. Clinically, aGCTs are the most common sex cord stromal cell tumors of the ovary and are characterized by increased estradiol levels. Surgery for the complete tumor resection is the basis for the treatment of primary and relapsed tumor. Chemotherapy treatment is administered only for advanced or nonresectable tumors. Most of the aGCTs are diagnosed at an early stage with a favorable prognosis. However, survival upon recurrence is modest in this pathology [18, 19]. The uniqueness of the $FOXL2^{C134W}$ mutation is a compelling finding in a tumor with an otherwise modestly impacted genome, which lacks the consistent induction of oncogenes or inactivation of tumor suppressor genes found among other tumor types. In fact, immunohistochemical evaluation of different oncogenes and tumor suppressors (*e.g.*, MYC, CDKN1A, ERBB2, and TP53) failed to detect a correlation with patient outcome [20]. Earlier studies have suggested that $FOXL2^{C134W}$ is potentially involved in the onset of aGCTs [15, 21–26], yet there is no clear mechanism to account for the causal relationship.

Foxo1 knockout mice showed embryonic lethality after embryonic day 10.5 [27, 28] owing to defects in vascularization and blood vessel formation, which precluded early studies of FOXO1 function in the ovary *in vivo*. More recently, the selective depletion of the *Foxo1* gene in mouse GCs revealed normal ovarian follicle morphology with subfertility, but there was no observation of tumorigenesis [29]. Similarly, mice with GC-specific depletion of the *Foxo3* gene also exhibited normal ovarian follicle morphology with no GC tumors (GCTs). However, large GCTs were developed in ~20% of the *Foxo1* and *Foxo3* double-knockout mice [29]. Moreover, the loss of *Foxo1*, *Foxo3*, and the tumor suppressor *Pten* in mouse GCs increased levels of estradiol and SMAD3 activation, and developed GCTs in 65% of female mice [30], ~10-fold higher than observed following targeted depletion of *Pten* alone [31]. Clinically, FOXO proteins are involved in various diseases, including cancer, diabetes mellitus, and Alzheimer's disease [32]. It is noteworthy that FOXO1 is targeted and inactivated by FHL2 and by the PI3K–AKT pathway; FHL2 is known as a transcriptional cosuppressor of FOXO1 and is implicated in aGCT aggression, whereas an elevated PI3K–AKT pathway is a hallmark of cancer [33]. Collectively, FOXO1 is considered a tumor suppressor that limits cell proliferation and induces apoptosis [34, 35].

We recently investigated the role of $FOXL2^{C134W}$ mutation in GC function with a hypothesis that $FOXL2^{C134W}$ regulates the expression of aGCT markers differently from $FOXL2^{wt}$. Specifically, we investigated FOXL2 regulation of inhibin B and CYP19 using a recently established human GC line, human GC line (HGrC1) [36]. The results showed that neither $FOXL2^{wt}$ nor $FOXL2^{C134W}$ regulates *Inhbb* expression levels when cells were treated

with or without activin A, or in the presence or absence of SMAD3 overexpression. However, $FOXL2^{C134W}$, but not $FOXL2^{wt}$, was able to induce CYP19 expression selectively in the presence of activin A or overexpressed SMAD3. Moreover, $FOXL2^{C134W}$ interactions with SMAD3 and with the FOX binding element (FBE) located at −199 bp upstream of the ATG initiation codon of human CYP19 were more sustainable than $FOXL2^{wt}$.

To extend our studies on the role of $FOXL2^{C134W}$ in regulating CYP19 expression via enhanced recruitment of SMAD3 to a proximal FBE, we have now assessed whether another forkhead protein, FOXO1, is involved in the mechanism because it was demonstrated to partner with SMAD3 in the regulation of activin induction of *Fshb* in immortalized murine LβT2 gonadotrope cells [37].

In this study, we have shown the actions and interactions of three factors potentially involved in the regulation of an aGCT marker, CYP19, namely SMAD3, FOXL2, and FOXO1 [26, 38, 39], following the hypothesis that FOXO1 can oppose $FOXL2^{C134W}$ actions. We have focused on whether and how FOXO1 differentially regulates $FOXL2^{C134W}$ and $FOXL2^{wt}$ activities on CYP19 expression and whether it occurs in association with SMAD3. It is remarkable that the finding of a new possible target, FOXO1, that modulates the function of $FOXL2^{C134W}$ has implications for both aGCT establishment and potential future modulation of the tumor. Certainly, new agents able to abolish the typical aGCT CYP19 upregulation appear to be important in the field of hormone-dependent cancer.

1. Materials and Methods

A. Plasmids and Reagents

Antibodies against FOXO1 (catalog no. 9454, RRID:AB_823503) [40], SMAD2/3 (catalog no. 3102, RRID:AB_10698742) [41], and β-actin (catalog no. 4967, RRID:AB_330288) [42] were purchased from Cell Signaling Technology (Danvers, MA); the antibody against FOXL2 (catalog no. IMG-3228, RRID:AB_613022) [43] was from Imgenex (San Diego, CA); the antibody against c-Myc tag (catalog no. 551101, RRID:AB_394046) [44] was from BD Pharmingen (Franklin Lakes, NJ); and the antibody against FLAG tag (catalog no. F1804, RRID:AB_262044) [45] was from Sigma-Aldrich (St. Louis, MO). Activin A was previously made in our laboratory and reported [46]. HGrC1 cells were established as previously described [36]. Expression plasmids encoding N-terminally Flag-tagged $hFOXO1^{wt}$ (catalog no. 13507), N-terminally Flag-tagged $hFOXO1^{3A}$ (catalog no. 13508), and N-terminally Flag-tagged $hFOXO1^{3A\text{-}DBD}$ (catalog no. 10696) were purchased from Addgene (Cambridge, MA). $FOXO1^{3A}$ has Ala residue substitutions at Thr24, Ser256, and Ser319 and is thus constitutively active whereas $FOXO1^{3A\text{-}DBD}$ lacks the DNA binding site of $FOXO1^{3A}$. N-terminally Flag-tagged human $FOXL2^{wt}$ ($FOXL2^{wt}$) was provided by Dr. Louise Bilezikjian [47], and its mutant ($FOXL2^{C134W}$) was made in our laboratory as previously reported [48, 49]. The expression plasmids encoding human SMAD3 with or without N-terminal Myc tag were prepared from those provided by Drs. Kohei Miyazono [50, 51] and Louise Bilezikjian [47]. Luciferase reporter plasmids of human CYP19 promoter in different lengths were made in our laboratory using PCR-based methods. Biotinylated oligonucleotide probes were purchased from Integrated DNA Technologies (San Diego, CA).

B. HGrC1 Cell Culture

HGrC1 cell properties and derivation were described earlier [52]. Notably, these cells bear two normal alleles of the *FOXL2* gene [52]. Cells were cultured in a standard incubator at 37°C in DMEM-F12 medium (catalog no. 12400-024, Thermo Fisher Scientific, Waltham, MA) complemented with antibiotics (penicillin and streptomycin) and 10% fetal bovine serum (catalog no. F6178, Sigma-Aldrich). HGrC1 cells at passage 14 were used for all of the experiments in this study. For some experiments, HGrC1 cells were treated with 100 ng/mL activin A for 24 hours in serum-free DMEM-F12 medium.

C. Transient Transfections

HGrC1 cells were cultured into either 12-well tissue culture plates (0.5×10^6 cells per well) or six-well tissue culture plates (1×10^6 cells per well). Medium was replaced the day after with serum-free DMEM-F12 (complemented with antibiotics), and transfection was performed using the above-described plasmids for 4 hours with Lipofectamine LTX with Plus or Lipofectamine 3000 reagents (catalog no. 15338100 or no. L3000008, respectively, Thermo Fisher Scientific) following the manufacturer's procedures. After 4 hours, medium was replaced with new serum-free DMEM-F12 and transfected cells were cultured at 37°C for 24 hours with or without activin A. At this point cells were lysed for further analyses.

D. RNA Extractions and Quantitative RT-PCR

After 4 hours of transfection and additional culture for 24 hours in serum-free DMEM-F12, HGrC1 cells were lysed using TRIzol reagent (catalog no. 15596026, Thermo Fisher Scientific) and RNA was extracted with a Direct-zol RNA MiniPrep kit (catalog no. R2052, Zymo Research, Irvine, CA) following the manufacturer's protocol. A high-capacity cDNA reverse transcription kit (catalog no. 4368814, Thermo Fisher Scientific) was used to reverse transcribe 1 μg of RNA. mRNA expression was quantified by qRT-PCR amplification of cDNA using SYBR Green PCR master mix (catalog no. 4309155, Thermo Fisher Scientific) and the ABI 7300 real-time PCR system thermal cycler from Applied Biosystems (Foster City, CA). The primer sequences used to amplify CYP19 were: forward, 5′-GGAATTATGAGGGCACATCC-3′, reverse, 5′-GTTGTAGTAGTTGCAGGCAC-3′; for L19: forward, 5′-GGGATTTGCATTCAGAGATCAG-3′, reverse, 5′-GGAAGGGCATCTCGTAAG-3′. Target gene expression was normalized on L19 expression.

E. Western Blot Analysis

After 4 hours of transfection and additional culture for 24 hours in serum-free DMEM-F12, HGrC1 cells were lysed in lysis buffer (RIPA buffer, catalog no. 89901, Thermo Fisher Scientific), phosphatase inhibitor cocktail (catalog no. 78420, Thermo Fisher Scientific), and protease inhibitor cocktail (catalog no. P8340, Sigma-Aldrich), and a Pierce bicinchoninic acid protein assay kit was used for total protein quantification (catalog no. 23227, Thermo Fisher Scientific). NuPAGE lithium dodecyl sulfate sample buffer 4× (catalog no. NP0007, Thermo Fisher Scientific) and β-mercaptoethanol (catalog no. 6010, Calbiochem, Billerica, MA) were added to cell lysates, and samples were denaturized at 95°C for 5 minutes. Protein separation occurred on 12% SDS-PAGE gels and with subsequent transfer to nitrocellulose membranes. Membranes were then incubated for 1 hour with blocking solution (BSA, catalog no. A30075-100, Research Products International, Mount Prospect, IL), and with primary antibodies overnight at 4°C. Membranes were washed three times, then incubated for 1 hour with horseradish peroxidase–conjugated secondary antibodies, further washed three more times, and incubated with SuperSignal West Femto maximum sensitivity substrate to detect chemiluminescence (catalog no. 34095, Thermo Fisher Scientific). Alternatively, primary and secondary antibodies incubations were performed using solutions 1 and 2, respectively, of Signal Enhancer HIKARI (catalog no. NU00101 and no. NU00102, Nacalai USA, San Diego, CA) to enhance protein detection. β-Actin was used as a loading control.

F. Luciferase Reporter Assay

After 4 hours of transfection and additional culture for 24 hours in serum-free DMEM-F12, HGrC1 cells (0.5×10^6 cells per sample) were lysed in a solution composed of 100 mM potassium phosphate (pH 7.8) and 0.2% Triton X-100. A luciferase reporter assay was performed with a Nano-Glo® Dual-Luciferase® reporter assay system (catalog no. N1610, Promega) following the manufacturer's instructions. The FLUOstar Omega microplate reader (BMG Labtech, Ortenberg, Germany) was used to measure the relative firefly

luciferase activity, which was normalized by β-galactosidase activity. We used the same plasmid constructs as reported in our earlier studies [52].

G. Coimmunoprecipitation and Oligonucleotide Binding Assays

After 4 hours of transfection and additional culture for 24 hours in serum-free DMEM-F12, HGrC1 cells (2.5×10^6 cells per sample for coimmunoprecipitation assay; 5×10^6 cells per sample for oligonucleotide binding assay) were lysed in lysis solution [25 mM Tris-HCl (pH 7.4), 140 mM NaCl, 1 mM EDTA, 0.1% Nonidet P-40, 0.5% Triton X-100, 10% glycerol, 2 mM NaF, freshly added 1 mM $Na_4P_2O_7$, protease inhibitor cocktail (catalog no. P8340, Sigma-Aldrich) and Benzonase (catalog no. E1014, Sigma-Aldrich)]. Cell extracts were then sonicated for 3 to 4 seconds twice, spun down at 4°C for 10 minutes at 13,000 rpm, and supernatants were collected. For the oligonucleotide binding assay, the EpiQuik™ general protein–DNA binding assay kit (catalog no. P-2004-96, EpiGentek, Farmingdale, NY) was used. For coimmunoprecipitation assays, supernatants were first precleared for 1 hour with mouse IgG agarose (catalog no. A0919) and immunoprecipitated using anti-FLAG M2 affinity gel (catalog no. A2220, Sigma-Aldrich) overnight at 4°C. The precipitants were washed three times in lysis buffer and eluted with FLAG peptide (catalog no. F3290, Sigma-Aldrich). After the elution step, immunoblot analysis of the samples was performed with c-myc antibody to detect the immunoprecipitated proteins tagged with cMyc. Secondary antibodies, goat anti-mouse IgG antibody (IRDye 800CW, LI-COR Biosciences, Lincoln, NE, RRID AB_10793856) [53], and goat anti-rabbit IgG antibody (IRDye 800CW, LI-COR Biosciences, RRID AB_10796098) [54], which are conjugated to IR fluorescent dyes excitable at 800 nm, were used to visualize the desired antigens using an 800-nm laser scanner (Odyssey, LI-COR Biosciences).

H. Statistical Analysis

All statistical analyses were performed using GraphPad Prism software. Data analysis was also performed with JMP Pro 12 software (SAS Institute, Cary, NC) using Box–Cox transformation and one-way ANOVA analysis with a least-squares means Tukey honestly significant difference test or a least-squares means Student *t* test. Significance was set at $P < 0.05$, and data are shown as mean ± SEM. For experiments where variance was not similar between the groups being compared, a parametric unpaired *t* test with a Welch correction or nonparametric Kolmogorov–Smirnov test was used.

2. Results

A. FOXO1^{wt} Suppresses CYP19 mRNA Expression Induced by FOXL2^{C134W} and SMAD3 in HGrC1 Cells

HGrC1 cells were transfected with SMAD3 and FOXL2^{wt} or FOXL2^{C134W} in the presence or absence of FOXO1^{wt}, or the matched empty vectors as controls. Cell lysates were collected for immunoblot analysis. With this protocol, we have previously demonstrated expression levels of endogenous and exogenous SMAD3, FOXL2^{wt}, and FOXL2^{C134W} [52]. Figure 1A shows expression levels of endogenous (empty vector) and exogenous FOXO1 (upper panel) and β-actin (lower panel). Total RNA was collected in parallel to evaluate CYP19 mRNA expression by qRT-PCR. Previously [52], we showed that SMAD3 or FOXL2^{wt} alone or in combination have indistinguishable effects on CYP19 mRNA expression from empty vector controls, whereas the combination of SMAD3 and FOXL2^{C134W} markedly induces CYP19 mRNA expression. The current study confirms the induction of CYP19 mRNA expression by SMAD3 with FOXL2^{C134W} (17-fold, Fig. 1B). Strikingly, a dramatic reduction (4.5-fold) of CYP19 mRNA expression was observed in the presence of FOXO1^{wt}. These results suggest

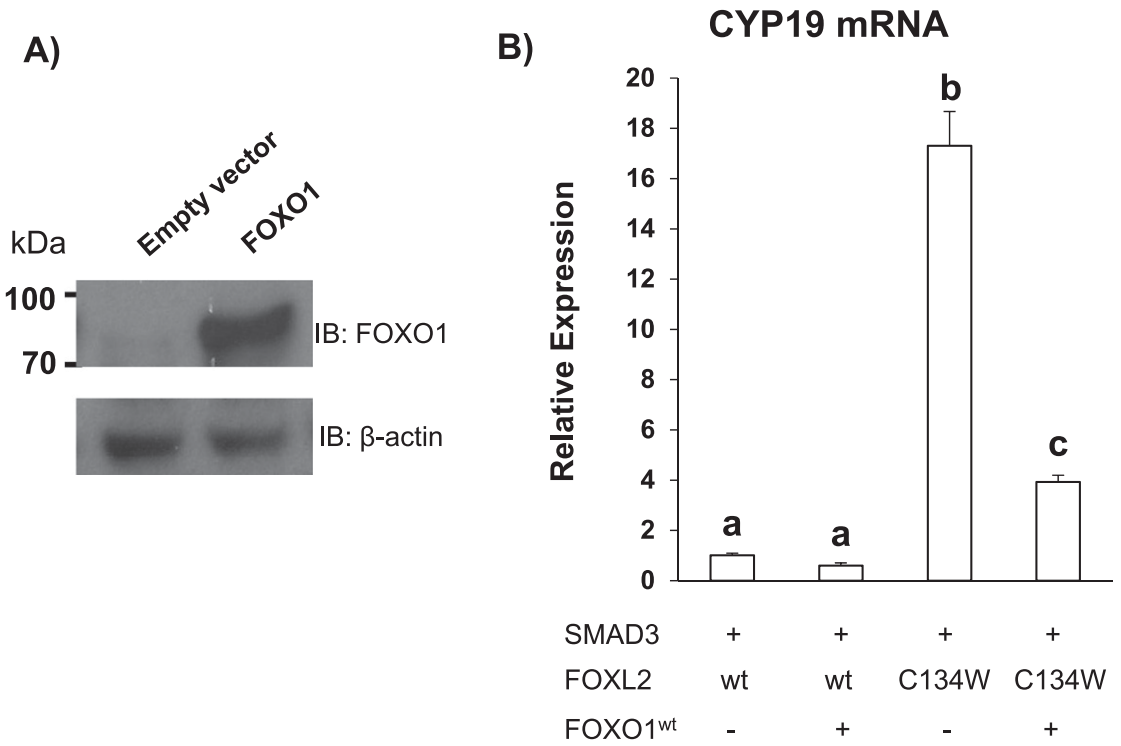

Figure 1. Effect of FOXO1 on SMAD3- and FOXL2^{C134W}-induced CYP19 mRNA expression in HGrC1 cells. HGrC1 cells were transfected with 500 ng of SMAD3, Flag-FOXL2^{wt}, Flag-FOXL2^{C134W}, and Flag-FOXO1^{wt} plasmids as shown, or their empty vectors to equalize the amount of plasmid transfected per well. After 4 h, serum-free medium was replaced and cells were cultured for 24 h, followed by the collection of cell lysates and total RNA. (A) Cell lysates were subjected to western blot analysis to show the expression levels of Flag-FOXO1^{wt} proteins. The expression levels of FOXL2 and SMAD3 in these cells were reported earlier [52]. Antibodies against FOXO1 and β-actin (for loading control) were used. Representative results from duplicate experiments are shown. (B) qRT-PCR was performed to measure CYP19 mRNA levels. Representative results (n = 3) from triplicate experiments are presented. Data are shown as mean ± SEM. Different letters denote significant difference among experimental conditions ($P < 0.05$).

that FOXO1 has a selective inhibitory role on CYP19 mRNA expression induced by SMAD3 and FOXL2^{C134W} in HGrC1 cells.

B. FOXO1^{3A} Abolishes SMAD3 and FOXL2^{C134W}-Induced CYP19 mRNA Expression

To approach the mechanism by which FOXO1 inhibits SMAD3- and FOXL2^{C134W}-induced CYP19 mRNA expression, we next tested the effect of the FOXO1^{3A} mutant that is confined to the nucleus and is thereby constitutively active [55]. As an additional control, we included the FOXO1$^{3A\text{-}DBD}$ mutant in this study, which lacks the capacity to bind SMAD3 as well as DNA [37].

HGrC1 cells were transfected with SMAD3 with different combinations of FOXL2^{wt}, FOXL2^{C134W}, FOXO1^{3A}, and FOXO1$^{3A\text{-}DBD}$ plasmids, or matched empty vectors as a control for total DNA transfected. Figure 2A shows the relative expression levels of endogenous (empty vector) and exogenous mutant FOXO1 proteins (upper panel) and β-actin (lower panel). Notably, FOXO1^{3A} showed a more slowly migrating band compared with endogenous FOXO1 due to the Flag tag. In FOXO1$^{3A\text{-}DBD}$, the Flag tag is offset by the deletion of 13 amino acids (amino acid positions from 208 to 220) from the DNA binding domain. Total RNA was again collected in parallel to evaluate CYP19 mRNA expression by qRT-PCR (Fig. 2B). Appreciably, while addition of FOXO1^{3A} or FOXO1$^{3A\text{-}DBD}$ to SMAD3 and FOXL2^{wt} did

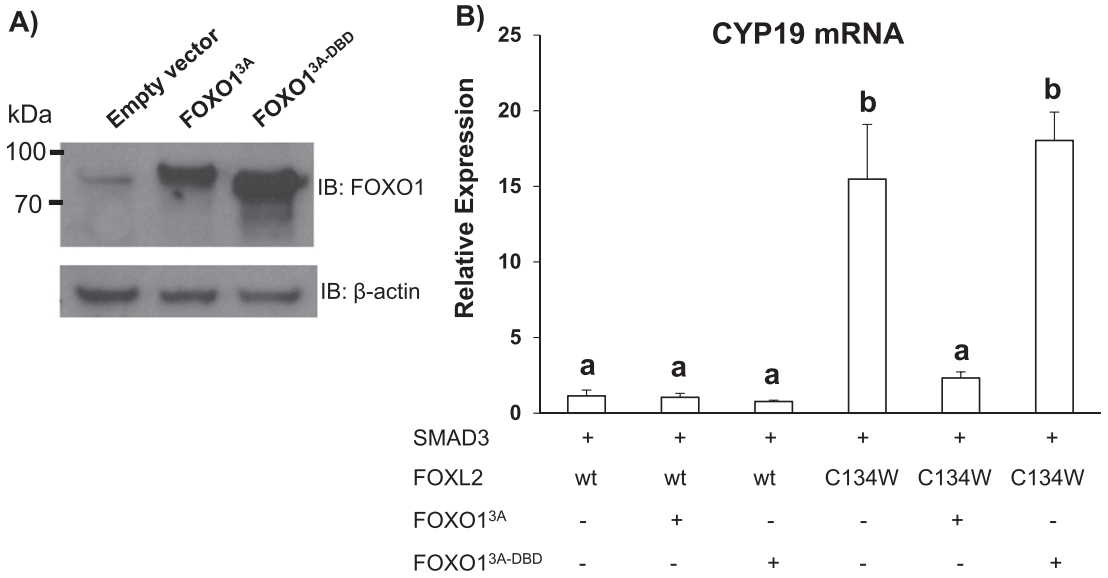

Figure 2. Effects of FOXO1^{3A} and FOXO1$^{3A\text{-}DBD}$ on SMAD3- and FOXL2^{C134W}-induced CYP19 mRNA expression in HGrC1 cells. HGrC1 cells were transfected with or without 500 ng of SMAD3, Flag-FOXL2^{wt}, Flag-FOXL2^{C134W}, Flag-FOXO1^{3A}, and Flag-FOXO1$^{3A\text{-}DBD}$ plasmids, alone or in combination. Empty expression vectors for FOXO1^{3A} and for FOXO1$^{3A\text{-}DBD}$ were added as necessary to equalize the amount of plasmid transfected per well. After 4 h, serum-free medium was replaced and cells were cultured for 24 h, followed by the collection of cell lysates and total RNA. (A) Cell lysates were subjected to western blot analysis to show the expression levels of FOXO1^{3A} and for FOXO1$^{3A\text{-}DBD}$ proteins using antibodies raised against FOXO1 or β-actin (for loading control). Representative results from duplicate experiments are shown. (B) qRT-PCR was performed to measure CYP19 mRNA levels. Representative results (n = 3) from triplicate experiments are presentedData are shown as mean ± SEM. Different letters denote significant difference among experimental conditions ($P < 0.05$).

not alter the CYP19 mRNA expression, FOXO1^{3A} abolished the SMAD3 and FOXL2^{C134W} induction (13-fold) of CYP19 expression down to control levels, indicating that the nuclear localization of FOXO1 is essential to suppress the cooperative induction of CYP19 by FOXL2^{C134W} and SMAD3. FOXO1$^{3A\text{-}DBD}$ did not exhibit any effects on SMAD3 and FOXL2^{C134W}-induced CYP19 mRNA expression, possibly due to its incapacity to bind SMAD3 and/or DNA.

C. FOXO1^{3A} Significantly Reduces CYP19 Promoter Activity Induced by SMAD3 and FOXL2^{C134W}

Using the Universal PBM Resource for Oligonucleotide Binding Evaluation database [56] to identify potential binding sites for FOX and SMAD proteins, five FBEs (FBE1 to FBE5) and one SMAD binding element (SBE) were found within 1 kb upstream of the translation start site in human CYP19 promoter [52] (Fig. 3A). A luciferase reporter plasmid was used with a sequence of 823 bp including the five potential FBE and one potential SBE sites, designated −823/CYP19-Luc as reported previously [52] (Fig. 3B). The relative luciferase activity of −823/CYP19-Luc in HGrC1 cells transfected with combinations of SMAD3, FOXL2^{C134W}, and FOXO1^{3A} plasmids (or matched empty vectors) is shown in Fig. 3C. We confirmed that the expression of FOXL2^{C134W} with SMAD3 increased CYP19 promoter activity, replicating past results that the combination (but not SMAD3 alone) could activate CYP19 promoter activity [52]. However, the coexpression of FOXO1^{3A} completely depressed −823/CYP19-Luc activity to control levels. These data together suggest that induction of CYP19 expression by FOXL2^{C134W} and SMAD signaling is opposed by FOXO1 at a transcriptional level.

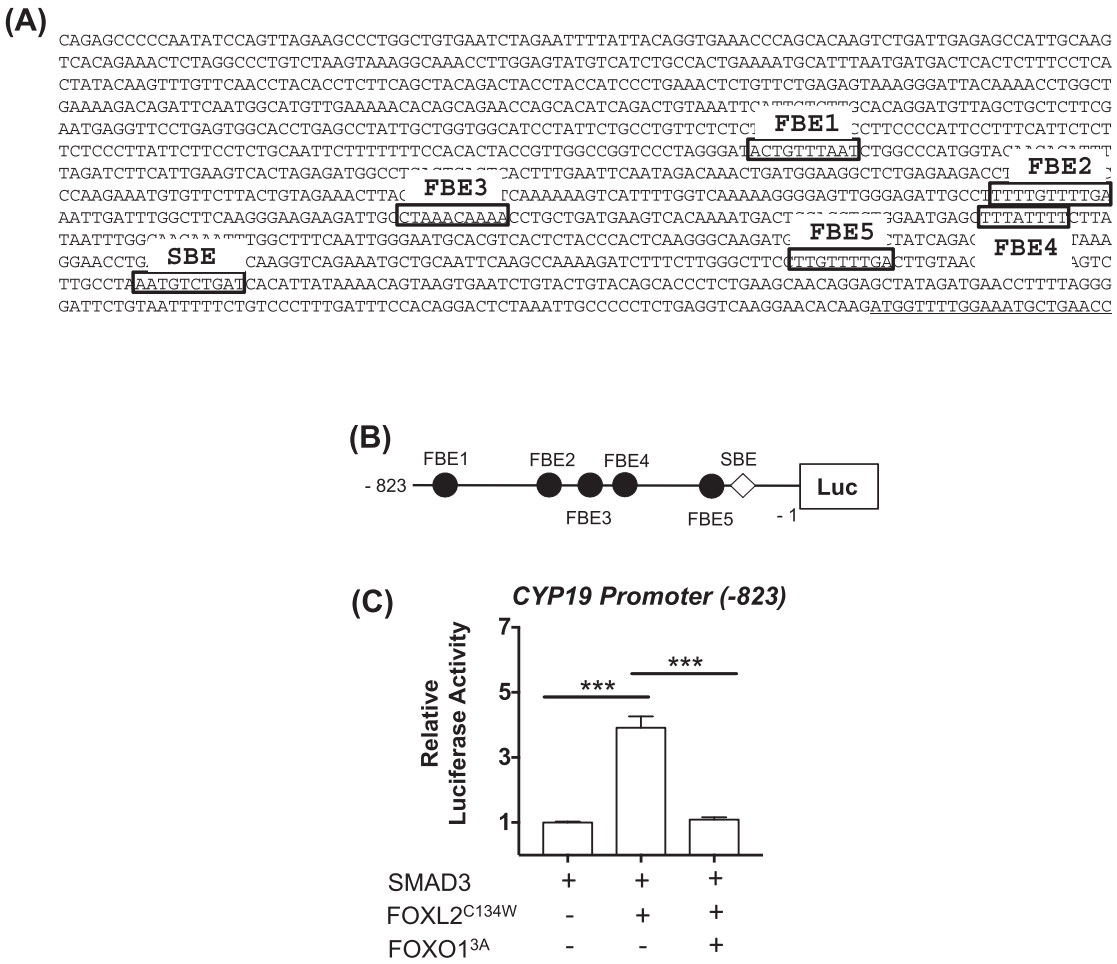

Figure 3. Human CYP19 promoter activity regulated by FOXL2 and FOXO1. (A) DNA sequences for potential binding sites of FOX (FBE1 to FBE5) and SMAD (SBE) proteins within 1 kb of the proximal region of human CYP19 promoter. (A) Human CYP19 promoter (1 kb) was explored by the Universal PBM Resource for Oligonucleotide Binding Evaluation database that includes data generated by universal protein binding microarray technology on the *in vitro* DNA binding specificities of proteins. The coding sequence of hCYP19 is underlined. (B) Luciferase reporter of human CYP19 promoter (−823/CYP19-Luc). Potential FOX (FBE1 to FBE5) and SMAD (SBE) binding sites are shown. HGrC1 cells were transfected with the −823/CYP19-Luc reporter and combinations of SMAD3, Flag-FOXL2^{C134W}, and Flag-FOXO1^{3A} plasmids. Empty expression vectors were added as necessary to equalize the amount of DNA transfected per well. After 4 h, serum-free medium was replaced and cells were cultured for 24 h, followed by collection of cell lysates. (C) Relative luciferase activities are shown. Representative results (n = 3) from triplicate experiments are presented. Data are shown as mean ± SEM and are analyzed using the two-tailed Mann−Whitney test. ***$P < 0.001$ for difference among experimental conditions.

D. FBE5 (−199) and SBE (−163) Are Involved in FOXO1^{3A} Inhibition of CYP19 Promoter Activation by SMAD3 and FOXL2^{C134W}

To resolve the *cis* elements responsible for FOXO1 action on CYP19 promoter, the −823/CYP19-Luc reporter was truncated to obtain four shorter constructs (Fig. 4). Their activities were evaluated in HGrC1 cells transfected with FOXL2^{C134W} and SMAD3 with or without FOXO1^{3A} plasmids. All constructs except the most proximal (−56/CYP19-Luc) showed a significant inhibition of FOXL2^{C134W}-induced CYP19 promoter activation by FOXO1^{3A}. These data imply that either the FBE5 (−199), the SBE (−163) [52], or both elements are

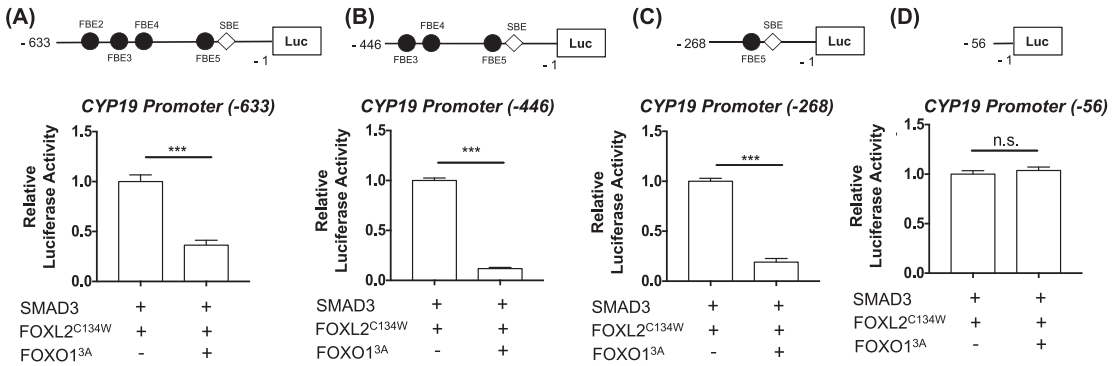

Figure 4. Luciferase activities of truncated human CYP19 promoters. (Upper panels) HGrC1 cells were transfected with an indicated CYP19-luciferase reporter (A, B, C or D) and combinations of SMAD3, Flag-FOXL2^{C134W} and Flag-FOXO1^{3A} plasmids. After 4 h, serum free medium was replaced, and cells were cultured for 24 h, followed by collection of cell lysates. (Lower panels) Ratio of relative luciferase activities on the effect of FOXL2^{C134W} or FOXO1^{3A} are shown. Representative results (n = 3) from triplicate experiments are presented. Data are shown as mean ± SEM and are analyzed using the two-tailed Mann-Whitney test. The asterisk denotes a significant difference among experimental conditions (***$P < 0.001$). n.s., not significant.

accountable for FOXO1 regulation of FOXL2^{C134W} activity (in the presence of an activated SMAD3 signaling) on the CYP19 promoter in HGrC1 cells.

E. FBE5 Is Required for FOXO1 to Inhibit FOXL2^{C134W} on CYP19 Transcription

Two further constructs were used from −823/CYP19-Luc reporter, namely an SBE mutant (Fig. 5A) and an FBE5 mutant (Fig. 5B) [52]. For the new constructs, six bases were mutated within the sequence of each binding element and the reporters were then tested for their activities. Interestingly, the SBE mutant (Fig. 5A) maintained significantly different activities between with or without FOXO1^{3A}, whereas the FBE5 mutant (Fig. 5B) failed to show inhibition by FOXO1^{3A}, indicating that FBE5 is sufficient to for FOXO1^{3A}-mediated reduction of CYP19 promoter activity induced by FOXL2^{C134W}. These data suggested that FOXO1^{3A} can inhibit FOXL2 ^{C134W} binding to CYP19 promoter, but also opened the question of whether this activity was due to a competitive action of FOXO1^{3A} for FOXL2 ^{C134W} binding to the FBE5 site or to SMAD3.

F. FOXO1 Associates With SMAD3 in HGrC1 Cells

Despite the lack of contribution of the SBE in the role of FOXO1 attenuation of FOXL2^{C134W} activity, our earlier [52] and current studies implicate SMAD3 as a critical FOXL2^{C134W} partner for CYP19 expression. In fact, SMAD3 forms a more stable protein complex with FOXL2^{C134W} than does FOXL2^{wt} in HGrC1 cells [52]. To investigate whether FOXO1 interacts with SMAD3, cells were transfected with combinations of SMAD3, FOXL2^{C134W}, and FOXO1^{3A} plasmids, and coimmunoprecipitation assays were performed. Figure 6 shows the input levels of SMAD3, FOXL2^{C134W}, and FOXO1^{3A} (top three panels) and the levels of SMAD3 coprecipitated with FOXL2^{C134W} or FOXO1^{3A} (bottom panel). Interestingly, FOXO1^{3A}, similar to FOXL2^{C134W}, associates with SMAD3, consistent with the putative role of SMAD3 in regulating FOXO1 activity [37].

G. FOXO1^{3A} Does Not Bind to FBE5 in HGrC1 Cells

We previously reported that FOXL2^{C134W} in the presence of SMAD3 binds to the FBE5 site in the proximal region of CYP19 promoter [52]. To investigate whether FOXO1 competes with FOXL2 to bind to the FBE5 site, we performed oligonucleotide binding assays using probes

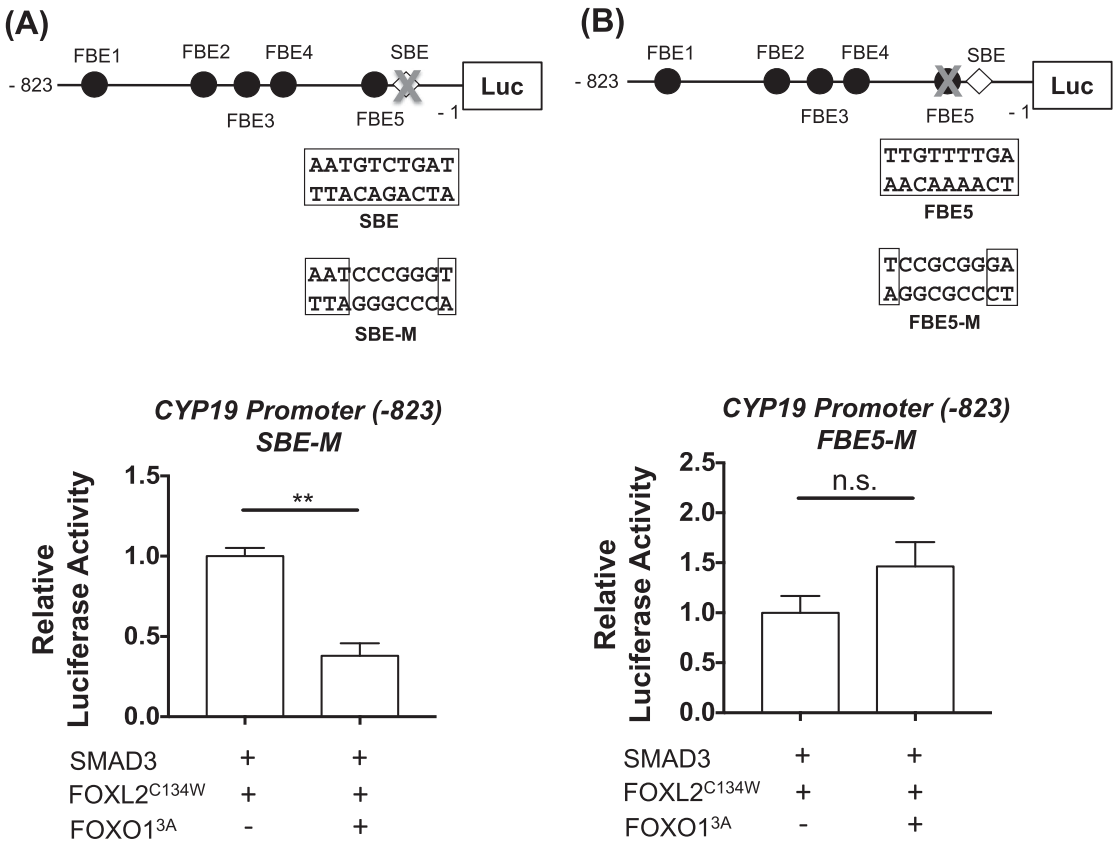

Figure 5. Contribution of FBE5 or SBE sites to FOXL2^{C134W} and FOXO1^{3A} activation of CYP19 transcription. SBE (A) and FBE5 (B) sites were mutated at six internal bases as indicated within the −823/CYP19-luciferase reporter, and HGrC1 cells were transfected with these constructs with combinations of SMAD3, Flag-FOXL2^{C134W}, and Flag-FOXO1^{3A} plasmids. After 4 h, serum-free medium was replaced and cells were cultured for 24 h, followed by collection of cell lysates. Relative luciferase activities are shown. Representative results (n = 3) from triplicate experiments are presented. Data are shown as mean ± SEM. Data are shown as mean ± SEM and are analyzed using the two-tailed Mann–Whitney test. $^{**}P < 0.01$ for difference among experimental conditions. n.s., not significant.

containing the FBE5 and SBE sites (Fig. 7A). Cells were transfected with combinations of SMAD3, FOXL2^{C134W}, and FOXO1^{3A} plasmids and treated with activin A for the final 24 hours, then lysed and subjected to a binding assay. In this case, activin A treatment was used to establish a uniform activation of SMAD3 activity in HGrC1 cells as previously demonstrated [52]. Figure 7B confirms this previous observation; specifically, that FOXL2^{C134W} binds to the probe selectively in the presence of Smad3 [52]. In contrast, FOXO1^{3A} did not bind to the same probe. Importantly, FOXL2^{C134W} did not bind to the probe when cotransfected with FOXO1^{3A}. These findings suggest that FOXO1^{3A} acts to prevent FOXL2^{C134W} binding to the FBE5 site.

H. FOXO1^{3A} Sequesters SMAD3 From the FOXL2^{C134W}/SMAD3 Complex

To further understand FOXO1^{3A} action in the presence of SMAD3/FOXL2^{C134W}, activin A–treated cells expressing combinations of SMAD3, FOXL2^{C134W}, and FOXO1^{3A} plasmids were subjected to immunoprecipitation and Western blot analyses. Figure 8A shows that although the input levels of FOXO1^{3A} and FOXL2^{C134W} are comparable (top two panels), SMAD3 selectively coprecipitates with FOXO1^{3A} (bottom panel). These findings suggest a model in which SMAD3 preferentially associates with FOXO1^{3A} relative to FOXL2^{C134W}; therefore, FOXO1^{3A} opposes FOXL2^{C134W} due to sequestration of SMAD3, a critical partner essential for its regulation of CYP19 transcription.

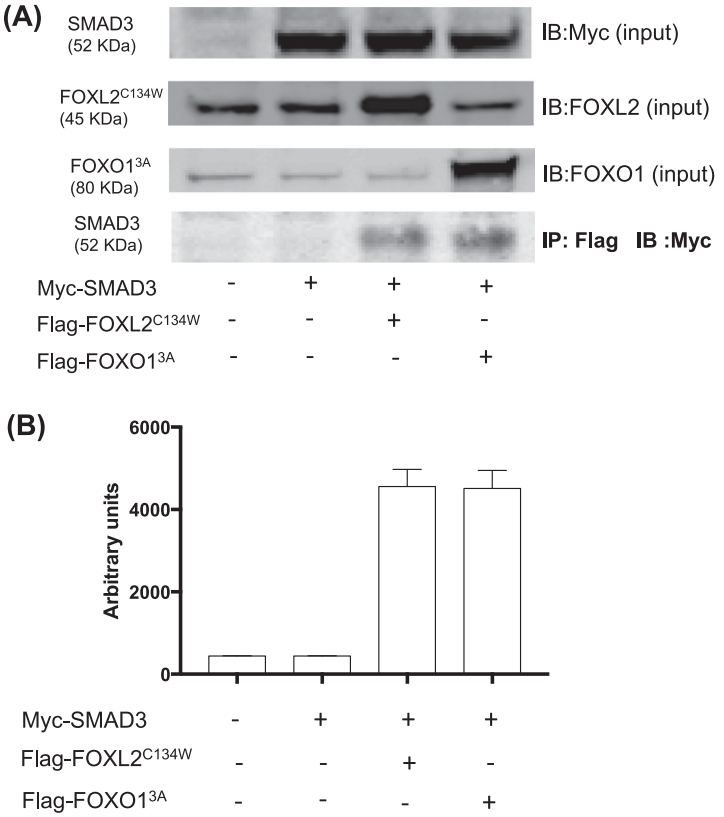

Figure 6. Protein–protein interactions between SMAD3 and FOXL2^{C134W} or FOXO1^{3A}. HGrC1 cells were transfected with combinations of Myc-SMAD3, Flag-FOXL2^{C134W}, and Flag-FOXO1^{3A} plasmids. Empty expression vectors were added as needed to equalize the amount of DNA transfected per well. After 4 h, serum-free medium was replaced and cells were cultured for 24 h, followed by collection of cell lysates. (A) INPUT levels of SMAD3, FOXL2, and FOXO1 proteins before immunoprecipitation were detected with anti-Myc, anti-FOXL2, and anti-FOXO1 antibodies respectively (top three panels). Protein lysates were immunoprecipitated with anti-Flag agarose beads, and SMAD3 proteins were detected with anti-Myc antibody (bottom panel). (B) Relative signal intensities of SMAD3 protein coprecipitated with FOXL2 and FOXO1 were measured. Representative results from triplicate experiments are presented. Data are shown as mean ± SEM.

3. Discussion

Ovarian cancer is the most lethal of gynecological malignances with a 5-year survival rate of 20% to 30% for patients with advanced disease [57]. GCTs account for ~5% of ovarian cancers, with an overall frequency of 1 per 100,000 women [58]. They can be divided into two subtypes, the rarer juvenile type and the more common adult type, based not only according to the differences of the age of the patients at their onset, but also by histology, nuclear morphology, and potential recurrence. Although juvenile GCTs can occur during infancy or puberty, they usually do not bear any FOXL2 mutation, and in fact, loss of FOXL2 expression is observed in more aggressive forms [59, 60]. In contrast, aGCTs, the most common type of GCTs, occur during perimenopausal and postmenopausal age, and almost all patients with aGCTs are heterozygous for the FOXL2^{C134W} mutation [16, 61]. Although most aGCTs are diagnosed at an early stage that can be treated with surgery, there is a high rate of recurrence, particularly among patients diagnosed at later stages [62], and 70% of patients with recurrence die as a result of GCTs. Traditional chemotherapy is relatively ineffective in women with advanced-stage or recurrent GCTs, which promotes the need for more effective therapeutic options for these patients. Additionally, as recurrent or metastatic tumors can manifest many years after removal of the primary tumor, with intervals up to 10 to 20 years not uncommon [63],

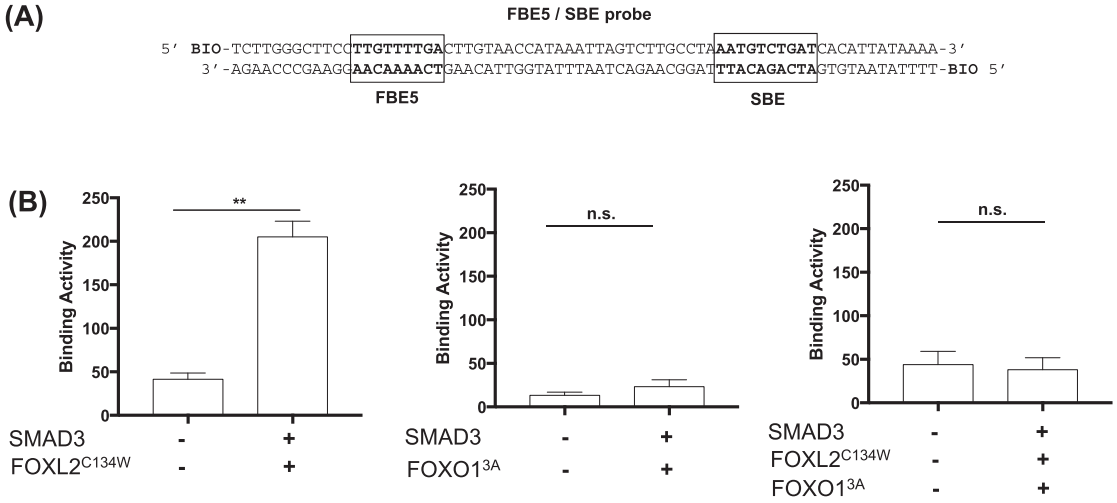

Figure 7. Oligonucleotide binding assay. (A) Biotinylated oligonucleotide probes were used. FBE5 and SBE sites are boxed. (B) HGrC1 cells were transfected with Flag-FOXL2^{C134W} or Flag-FOXO1^{3A} plus Myc-SMAD3 plasmids. Empty expression vectors were added as needed to equalize the amount of DNA transfected per well. After 4 h, serum-free medium was replaced and cells were cultured for 24 h in the presence of 100 ng/mL activin A, followed by collection of cell lysates. Protein lysates were incubated with the probe precoupled to streptavidin-conjugated agarose plates following procedures described in vendor protocol (see *Materials and Methods*), and FOXL2 and FOXO1 proteins were detected with an anti-Flag antibody. Relative signal intensities of FOXL2 and FOXO1 protein bound to streptavidin-conjugated probe were measured. Representative results from triplicate experiments are presented. Data are shown as mean ± SEM. $^{**}P < 0.01$ for difference among experimental conditions. n.s., not significant.

there is a need for a diagnostic marker to allow accurate assessment of recurrence risk during clinical follow-up of patients.

The FOXO transcription factors play crucial cellular processes by orchestrating programs of gene expression, including (i) initiation of apoptosis, (ii) promotion of cell cycle arrest, (iii) reactive oxygen species detoxification, (iv) repair of damaged DNA, and (v) facilitation of glucose metabolism and energy homeostasis [64]. In particular, their roles in the cell cycle arrest and the initiation of apoptosis support the role for FOXO factors as tumor suppressors. Our current finding in the present study may suggest that FOXO1 exerts its tumor-suppressive activity by limiting FOXL2^{C134W}-induced activity in CYP19 expression and consequently estradiol synthesis in GCs. FOXO1 is the most highly expressed FOXO family member in insulin-responsive tissues, where insulin signaling through the PI3K–AKT pathway plays a key regulation of FOXO1 activities [65]. Indeed, FOXO1 activities are regulated through phosphorylation at Thr24, Ser256, and Ser319 in response to the PI3K–AKT signaling, resulting in translocation of the factors outside the nucleus and their consequent inactivation [66]. Following nuclear exclusion, FOXO1 maintains its inactive state and is subject to ubiquitination and subsequent proteasomal degradation. The activation of PI3K–AKT signaling is common across many tumor types [67]. The inactivation of FOXO1 in response to PI3K represents one mechanism by which tumor cells avoid cell cycle arrest and apoptosis [68].

In the present study, we describe a novel role for the transcription factor FOXO1 in the inhibition of CYP19 expression induced by the synergistic action of mutant FOXL2^{C134W} and its cofactor SMAD3. However, FOXO1 showed no effect on FOXL2^{wt} action, indicating that FOXO1 has an inhibitory role selectively on FOXL2^{C134W}-induced CYP19 expression in the presence of SMAD3.

Our experimental approach to address the underlying molecular mechanism showed that FOXO1 competes with FOXL2^{C134W} in binding the essential cofactor SMAD3. Data showed that SMAD3 sequestration by FOXO1^{3A} appeared to be the main molecular event upstream of the FOXO1 reversal of the CYP19 upregulation by the FOXL2^{C134W}/SMAD3 complex. This

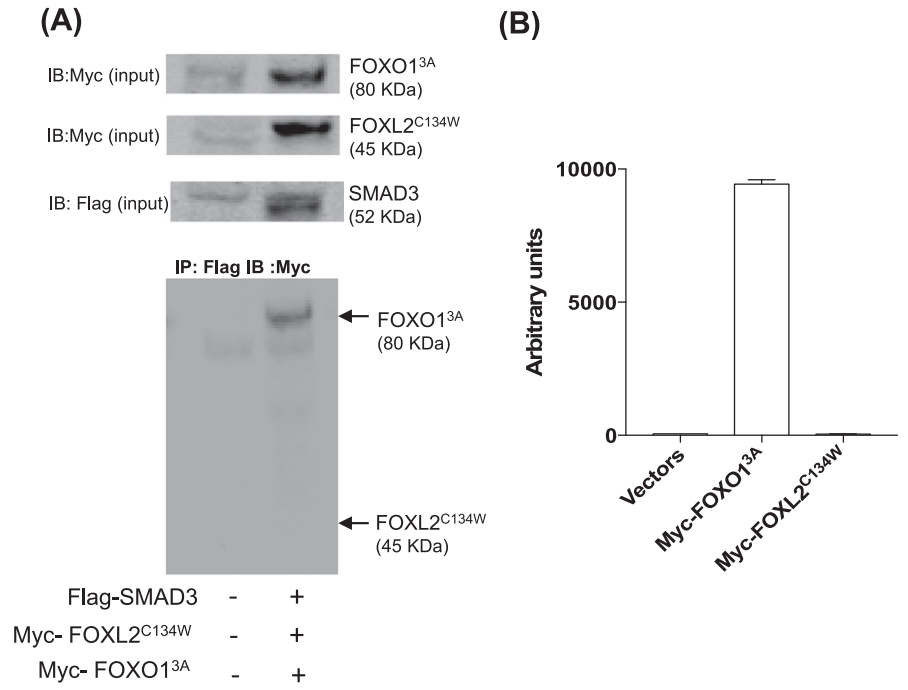

Figure 8. Competitive interactions between SMAD3 and FOXL2^{C134W} or FOXO1^{3A}. HGrC1 cells were transfected with combinations of Flag-SMAD3, Myc-FOXL2^{C134W}, and Myc-FOXO1^{3A} plasmids. Empty expression vectors were added as needed to equalize the amount of DNA transfected per well. After 4 h, serum-free medium was replaced and cells were cultured for 24 h in the presence of 100 ng/mL activin A, followed by collection of cell lysates. (A) Protein lysates were immunoprecipitated with anti-Flag agarose beads, and FOXO1 and FOXL2 proteins were detected with anti-Myc antibody. Input levels of SMAD3, FOXL2, and FOXO1 proteins before immunoprecipitation were detected with anti-Flag and anti-Myc antibodies, respectively. (B) Relative signal intensities of FOXL2 and FOXO1 protein coprecipitated with SMAD3 were measured. Representative results from triplicate experiments are presented. Data are shown as mean ± SEM.

finding is in good accord with reports by others that FOXO1 partners with SMAD3 in other physiological and pathological conditions [69, 70]. For example, in hepatocytes, TGF-β1/Smad3 promotes gluconeogenesis via the PP2A–AMPK–FOXO1 pathways during fasting/feeding as well as during pathologic conditions such as insulin resistance and diabetes [71]. Similarly, SMAD3/4 and FOXO1 have essential functions in oligodendrocyte differentiation [72], and it was suggested in 2004 that the FOXO1/SMAD3 complex may control neuroepithelial and glioblastoma cell proliferation in brain tumors [73].

Consistent with these existing views of FOXO1 functions, FOXO1^{3A} in the current study exhibited more potent activity than did FOXO1^{wt}. Interestingly, the deletion of the DNA binding domain in FOXO1^{3A} (FOXO1$^{3A\text{-}DBD}$) compromised the inhibition of FOXL2^{C134W} by FOXO1, despite a lack of binding by FOXO1 to FBE5. Indeed, the DNA binding domain of FOXO1 is also essential for SMAD3 binding [37], further supporting a model in which FOXO1 directly competes with FOXL2^{C134W} for binding to SMAD3. FOXL2^{C134W} action at the FBE5 site on CYP19 promoter occurs with SMAD3 as a cofactor [52]. This is not broadly true of all SMADs, as SMAD2 [52] and other SMADs, including SMAD1, SMAD5, and SMAD8 (data not shown), fail to cooperate with FOXL2^{C134W} to regulate CYP19 transcription in HGrC1 cells. Given that FOXO1 does not bind to FBE5, but exhibits more stable interaction with SMAD3 than does FOXL2^{C134W}, we propose a model in which FOXO1 prevents DNA binding of FOXL2^{C134W} via a competition for SMAD3, and not for the same DNA binding site. We suggest a possible mechanism by which the FOXO1 sequestration of SMAD3 inhibits FOXL2^{C134W}/SMAD3-induced CYP19 expression in HGrC1 cells as depicted in Fig. 9. An inhibitory role for FOXO1 on CYP19 regulation was previously postulated by Park *et al.* [74]

using rat primary GCs by showing that a synergistic induction of FSH and activin A on CYP19 expression was supported by endogenous FOXO1 phosphorylation (thus inactivation) via the PI3K–AKT signaling activated by FSH whereas overexpression of $FOXO1^{3A}$ suppresses the synergistic induction.

In summary, we have used HGrC1 cells to investigate the role of FOXO1 in the regulation of CYP19 expression in opposition to $FOXL2^{C134W}$ mutant reported earlier [52]. Our findings are that (i) $FOXO1^{wt}$ decreases CYP19 mRNA expression cooperatively induced by $FOXL2^{C134W}$ and SMAD3, and the constitutively active mutant $FOXO1^{3A}$ is more potent but the $FOXO1^{3A\text{-}DBD}$ mutant has no effect because it does not bind SMAD3 [37], (ii) the above-observed regulation occurs at the transcriptional level, (iii) the presence of $FOXO1^{3A}$ prevents the $FOXL2^{C134W}$/SMAD3 complex binding to the FBE5 site in the proximal region of CYP19 promoter, and (iv) $FOXO1^{3A}$ interacts more strongly with SMAD3 but not with FBE5, suggesting that its inhibitory action is possibly related to a sequestration of SMAD3 by FOXO1. Based on our data and in accordance with the literature, these molecular events take place in the nucleus because $FOXO1^{3A}$ cannot be phosphorylated in the mutated residues and this prevents its translocation in the cytoplasm. Also, $FOXL2^{C134W}$ and SMAD3 are located in the nucleus as described in the literature [37, 75–77].

To our knowledge, this study is the first to demonstrate the ability of FOXO1 in restoring an altered CYP19 transcriptional activity by $FOXL2^{C134W}$ mutant. It is therefore conceivable

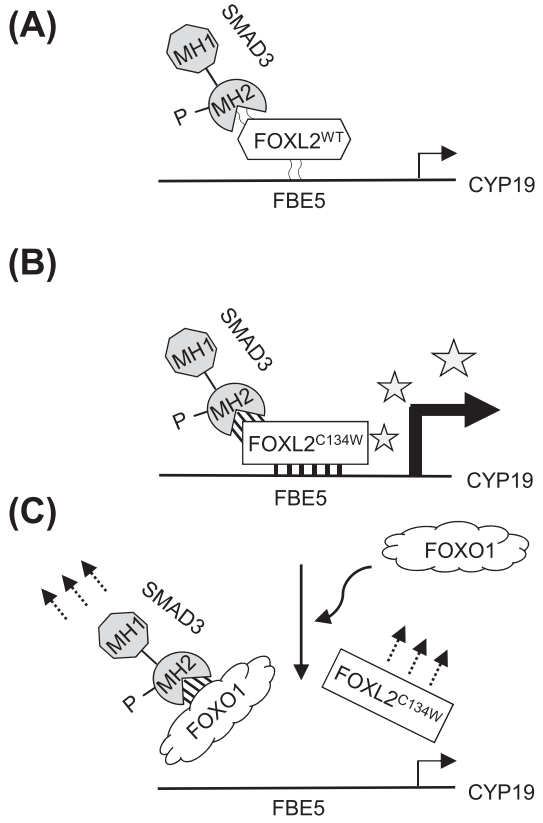

Figure 9. Possible molecular mechanism for the regulation of *CYP19* transcription by FOXO1 and $FOXL2^{C134W}$. (A) and (B) Findings of our previous study where $FOXL2^{C134W}$ and SMAD3 synergistically stimulate CYP19 transcription by binding to FBE5 in CYP19 promoter more strongly than $FOXL2^{wt}$ and SMAD3. (C) Data collected in this study show the ability of FOXO1 to counteract the synergistic activity of $FOXL2^{C134W}$ and SMAD3 in the stimulation of CYP19 transcription. FOXO1 and $FOXL2^{C134W}$ both bind SMAD3, but FOXO1 does it more strongly than $FOXL2^{C134W}$. Therefore, FOXO1 negates the ability of $FOXL2^{C134W}$ to bind SMAD3 and thus to enhance a steady-state level of *CYP19* transcription.

that FOXO1 acts as a tumor suppressor by preventing $FOXL2^{C134W}$ activity to enhance CYP19 expression, leading to estrogen access in women with aGCTs. Because the activity of FOXO1 is tightly regulated by posttranslational modifications, including phosphorylation, acetylation, and ubiquitylation [78], therapeutically targeting such modification steps could lead to the discovery and development of efficacious agents against aGCTs. In conclusion, this work addressed to one of the main features of aGCTs: the $FOXL2^{C134W}$-driven upregulation of aromatase expression and the subsequently increased estradiol levels in these patients. Our findings of the new possible target, FOXO1, that modulates the activity of $FOXL2^{C134W}$ appear to be important in the field of ovarian cancer because it has implications for both aGCT establishment and potential future modulation of the tumor.

Acknowledgments

The authors thank Dr. Varykina G. Thackray for providing us with Flag-$hFOXO1^{wt}$ and Flag-$hFOXO1^{3A}$ expression plasmids, Dr. Louise Bilezikjian for $FOXL2^{wt}$ expression plasmid, and Dr. Kohei Miyazono for providing us with the original hSMAD3 cDNA clones.

Financial Support: This work was supported by National Institutes of Health/National Institute of Child Health and Human Development Grant P50HD012303 (to S.S.) and by University of California San Diego Department of Reproductive Medicine Fund 60121B (to S.S.).

Additional Information

Correspondence: Shunichi Shimasaki, PhD, Department of Reproductive Medicine, School of Medicine, University of California San Diego, 9500 Gilman Drive, La Jolla, California 92093. E-mail: sshimasaki@ucsd.edu.

Disclosure Summary: The authors have nothing to disclose.

Data Availability: All data generated or analyzed during this study are included in this published article or in the data repositories listed in References.

References and Notes

1. Jackson BC, Carpenter C, Nebert DW, Vasiliou V. Update of human and mouse forkhead box (*FOX*) gene families. *Hum Genomics*. 2010;**4**(5):345–352.
2. Lehmann OJ, Sowden JC, Carlsson P, Jordan T, Bhattacharya SS. Fox's in development and disease. *Trends Genet*. 2003;**19**(6):339–344.
3. Golson ML, Kaestner KH. Fox transcription factors: from development to disease. *Development*. 2016; **143**(24):4558–4570.
4. Uhlenhaut NH, Treier M. Forkhead transcription factors in ovarian function. *Reproduction*. 2011; **142**(4):489–495.
5. Crisponi L, Deiana M, Loi A, Chiappe F, Uda M, Amati P, Bisceglia L, Zelante L, Nagaraja R, Porcu S, Ristaldi MS, Marzella R, Rocchi M, Nicolino M, Lienhardt-Roussie A, Nivelon A, Verloes A, Schlessinger D, Gasparini P, Bonneau D, Cao A, Pilia G. The putative forkhead transcription factor *FOXL2* is mutated in blepharophimosis/ptosis/epicanthus inversus syndrome. *Nat Genet*. 2001;**27**(2): 159–166.
6. Cocquet J, De Baere E, Gareil M, Pannetier M, Xia X, Fellous M, Veitia RA. Structure, evolution and expression of the FOXL2 transcription unit. *Cytogenet Genome Res*. 2003;**101**(3–4):206–211.
7. Cocquet J, Pailhoux E, Jaubert F, Servel N, Xia X, Pannetier M, De Baere E, Messiaen L, Cotinot C, Fellous M, Veitia RA. Evolution and expression of *FOXL2*. *J Med Genet*. 2002;**39**(12):916–921.
8. Ellsworth BS, Egashira N, Haller JL, Butts DL, Cocquet J, Clay CM, Osamura RY, Camper SA. FOXL2 in the pituitary: molecular, genetic, and developmental analysis. *Mol Endocrinol*. 2006;**20**(11): 2796–2805.
9. Loffler KA, Zarkower D, Koopman P. Etiology of ovarian failure in blepharophimosis ptosis epicanthus inversus syndrome: *FOXL2* is a conserved, early-acting gene in vertebrate ovarian development. *Endocrinology*. 2003;**144**(7):3237–3243.
10. Pisarska MD, Bae J, Klein C, Hsueh AJ. Forkhead L2 is expressed in the ovary and represses the promoter activity of the steroidogenic acute regulatory gene. *Endocrinology*. 2004;**145**(7):3424–3433.

11. Schmidt D, Ovitt CE, Anlag K, Fehsenfeld S, Gredsted L, Treier AC, Treier M. The murine winged-helix transcription factor Foxl2 is required for granulosa cell differentiation and ovary maintenance. *Development*. 2004;**131**(4):933–942.
12. Governini L, Carrarelli P, Rocha AL, Leo VD, Luddi A, Arcuri F, Piomboni P, Chapron C, Bilezikjian LM, Petraglia F. *FOXL2* in human endometrium: hyperexpressed in endometriosis. *Reprod Sci*. 2014; **21**(10):1249–1255.
13. Uda M, Ottolenghi C, Crisponi L, Garcia JE, Deiana M, Kimber W, Forabosco A, Cao A, Schlessinger D, Pilia G. *Foxl2* disruption causes mouse ovarian failure by pervasive blockage of follicle development. *Hum Mol Genet*. 2004;**13**(11):1171–1181.
14. Uhlenhaut NH, Jakob S, Anlag K, Eisenberger T, Sekido R, Kress J, Treier AC, Klugmann C, Klasen C, Holter NI, Riethmacher D, Schütz G, Cooney AJ, Lovell-Badge R, Treier M. Somatic sex reprogramming of adult ovaries to testes by FOXL2 ablation. *Cell*. 2009;**139**(6):1130–1142.
15. Leung DT, Fuller PJ, Chu S. Impact of FOXL2 mutations on signaling in ovarian granulosa cell tumors. *Int J Biochem Cell Biol*. 2016;**72**:51–54.
16. Shah SP, Köbel M, Senz J, Morin RD, Clarke BA, Wiegand KC, Leung G, Zayed A, Mehl E, Kalloger SE, Sun M, Giuliany R, Yorida E, Jones S, Varhol R, Swenerton KD, Miller D, Clement PB, Crane C, Madore J, Provencher D, Leung P, DeFazio A, Khattra J, Turashvili G, Zhao Y, Zeng T, Glover JN, Vanderhyden B, Zhao C, Parkinson CA, Jimenez-Linan M, Bowtell DD, Mes-Masson AM, Brenton JD, Aparicio SA, Boyd N, Hirst M, Gilks CB, Marra M, Huntsman DG. Mutation of *FOXL2* in granulosa-cell tumors of the ovary. *N Engl J Med*. 2009;**360**(26):2719–2729.
17. Zannoni GF, Improta G, Petrillo M, Pettinato A, Scambia G, Fraggetta F. FOXL2 molecular status in adult granulosa cell tumors of the ovary: a study of primary and metastatic cases. *Oncol Lett*. 2016; **12**(2):1159–1163.
18. Färkkilä A, Haltia UM, Tapper J, McConechy MK, Huntsman DG, Heikinheimo M. Pathogenesis and treatment of adult-type granulosa cell tumor of the ovary. *Ann Med*. 2017;**49**(5):435–447.
19. Khosla D, Dimri K, Pandey AK, Mahajan R, Trehan R. Ovarian granulosa cell tumor: clinical features, treatment, outcome, and prognostic factors. *N Am J Med Sci*. 2014;**6**(3):133–138.
20. King LA, Okagaki T, Gallup DG, Twiggs LB, Messing MJ, Carson LF. Mitotic count, nuclear atypia, and immunohistochemical determination of Ki-67, c-myc, p21-ras, c-erbB2, and p53 expression in granulosa cell tumors of the ovary: mitotic count and Ki-67 are indicators of poor prognosis. *Gynecol Oncol*. 1996;**61**(2):227–232.
21. Fleming NI, Knower KC, Lazarus KA, Fuller PJ, Simpson ER, Clyne CD. Aromatase is a direct target of FOXL2: C134W in granulosa cell tumors via a single highly conserved binding site in the ovarian specific promoter. *PLoS One*. 2010;**5**(12):e14389.
22. Benayoun BA, Anttonen M, L'Hôte D, Bailly-Bechet M, Andersson N, Heikinheimo M, Veitia RA. Adult ovarian granulosa cell tumor transcriptomics: prevalence of FOXL2 target genes misregulation gives insights into the pathogenic mechanism of the p.Cys134Trp somatic mutation. *Oncogene*. 2013;**32**(22): 2739–2746.
23. Anttonen M, Pihlajoki M, Andersson N, Georges A, L'hôte D, Vattulainen S, Färkkilä A, Unkila-Kallio L, Veitia RA, Heikinheimo M. FOXL2, GATA4, and SMAD3 co-operatively modulate gene expression, cell viability and apoptosis in ovarian granulosa cell tumor cells. *PLoS One*. 2014;**9**(1):e85545.
24. Kim JH, Kim YH, Kim HM, Park HO, Ha NC, Kim TH, Park M, Lee K, Bae J. FOXL2 posttranslational modifications mediated by GSK3β determine the growth of granulosa cell tumours. *Nat Commun*. 2014;**5**(1):2936.
25. Caburet S, Anttonen M, Todeschini AL, Unkila-Kallio L, Mestivier D, Butzow R, Veitia RA. Combined comparative genomic hybridization and transcriptomic analyses of ovarian granulosa cell tumors point to novel candidate driver genes. *BMC Cancer*. 2015;**15**(1):251.
26. Jamieson S, Fuller PJ. Molecular pathogenesis of granulosa cell tumors of the ovary. *Endocr Rev*. 2012; **33**(1):109–144.
27. Hosaka T, Biggs WH III, Tieu D, Boyer AD, Varki NM, Cavenee WK, Arden KC. Disruption of forkhead transcription factor (FOXO) family members in mice reveals their functional diversification. *Proc Natl Acad Sci USA*. 2004;**101**(9):2975–2980.
28. Furuyama T, Kitayama K, Shimoda Y, Ogawa M, Sone K, Yoshida-Araki K, Hisatsune H, Nishikawa S, Nakayama K, Nakayama K, Ikeda K, Motoyama N, Mori N. Abnormal angiogenesis in *Foxo1* (*Fkhr*)-deficient mice. *J Biol Chem*. 2004;**279**(33):34741–34749.
29. Liu Z, Castrillon DH, Zhou W, Richards JS. FOXO1/3 depletion in granulosa cells alters follicle growth, death and regulation of pituitary FSH. *Mol Endocrinol*. 2013;**27**(2):238–252.

30. Liu Z, Ren YA, Pangas SA, Adams J, Zhou W, Castrillon DH, Wilhelm D, Richards JS. FOXO1/3 and PTEN depletion in granulosa cells promotes ovarian granulosa cell tumor development. *Mol Endocrinol*. 2015;**29**(7):1006–1024.
31. Laguë MN, Paquet M, Fan HY, Kaartinen MJ, Chu S, Jamin SP, Behringer RR, Fuller PJ, Mitchell A, Doré M, Huneault LM, Richards JS, Boerboom D. Synergistic effects of *Pten* loss and WNT/CTNNB1 signaling pathway activation in ovarian granulosa cell tumor development and progression. *Carcinogenesis*. 2008;**29**(11):2062–2072.
32. Farhan M, Wang H, Gaur U, Little PJ, Xu J, Zheng W. FOXO signaling pathways as therapeutic targets in cancer. *Int J Biol Sci*. 2017;**13**(7):815–827.
33. Hua G, He C, Lv X, Fan L, Wang C, Remmenga SW, Rodabaugh KJ, Yang L, Lele SM, Yang P, Karpf AR, Davis JS, Wang C. The four and a half LIM domains 2 (FHL2) regulates ovarian granulosa cell tumor progression via controlling AKT1 transcription. *Cell Death Dis*. 2016;**7**(7):e2297.
34. Coomans de Brachène A, Demoulin JB. FOXO transcription factors in cancer development and therapy. *Cell Mol Life Sci*. 2016;**73**(6):1159–1172.
35. Fruman DA, Chiu H, Hopkins BD, Bagrodia S, Cantley LC, Abraham RT. The PI3K pathway in human disease. *Cell*. 2017;**170**(4):605–635.
36. Bayasula IA, Iwase A, Kiyono T, Takikawa S, Goto M, Nakamura T, Nagatomo Y, Nakahara T, Kotani T, Kobayashi H, Kondo M, Manabe S, Kikkawa F. Establishment of a human nonluteinized granulosa cell line that transitions from the gonadotropin-independent to the gonadotropin-dependent status. *Endocrinology*. 2012;**153**(6):2851–2860.
37. Park CH, Skarra DV, Rivera AJ, Arriola DJ, Thackray VG. Constitutively active FOXO1 diminishes activin induction of *Fshb* transcription in immortalized gonadotropes. *PLoS One*. 2014;**9**(11):e113839.
38. Fang X, Gao Y, Li Q. SMAD3 activation: a converging point of dysregulated TGF-beta superfamily signaling and genetic aberrations in granulosa cell tumor development? *Biol Reprod*. 2016;**95**(5):105.
39. Li J, Bao R, Peng S, Zhang C. The molecular mechanism of ovarian granulosa cell tumors. *J Ovarian Res*. 2018;**11**(1):13.
40. RRID:AB_823503, https://antibodyregistry.org/search?q=AB_823503.
41. RRID:AB_10698742, https://antibodyregistry.org/search?q=AB_10698742.
42. RRID:AB_330288, https://antibodyregistry.org/search?q=AB_330288.
43. RRID:AB_613022, https://antibodyregistry.org/search?q=AB_613022.
44. RRID:AB_394046, https://antibodyregistry.org/search?q=AB_394046.
45. RRID:AB_262044, https://antibodyregistry.org/search?q=AB_262044.
46. Otsuka F, Shimasaki S. A negative feedback system between oocyte bone morphogenetic protein 15 and granulosa cell kit ligand: its role in regulating granulosa cell mitosis. *Proc Natl Acad Sci USA*. 2002; **99**(12):8060–8065.
47. Blount AL, Schmidt K, Justice NJ, Vale WW, Fischer WH, Bilezikjian LM. FoxL2 and Smad3 coordinately regulate follistatin gene transcription. *J Biol Chem*. 2009;**284**(12):7631–7645.
48. McTavish KJ, Nonis D, Hoang YD, Shimasaki S. Granulosa cell tumor mutant $FOXL2^{C134W}$ suppresses GDF-9 and activin A-induced follistatin transcription in primary granulosa cells. *Mol Cell Endocrinol*. 2013;**372**(1-2):57–64.
49. Nonis D, McTavish KJ, Shimasaki S. Essential but differential role of $FOXL2^{wt}$ and $FOXL2^{C134W}$ in GDF-9 stimulation of follistatin transcription in co-operation with Smad3 in the human granulosa cell line COV434. *Mol Cell Endocrinol*. 2013;**372**(1-2):42–48.
50. Kawabata M, Inoue H, Hanyu A, Imamura T, Miyazono K. Smad proteins exist as monomers in vivo and undergo homo- and hetero-oligomerization upon activation by serine/threonine kinase receptors. *EMBO J*. 1998;**17**(14):4056–4065.
51. Komuro A, Imamura T, Saitoh M, Yoshida Y, Yamori T, Miyazono K, Miyazawa K. Negative regulation of transforming growth factor-β (TGF-β) signaling by WW domain-containing protein 1 (WWP1). *Oncogene*. 2004;**23**(41):6914–6923.
52. Belli M, Iwata N, Nakamura T, Iwase A, Stupack D, Shimasaki S. $FOXL2^{C134W}$-induced CYP19 expression via cooperation with SMAD3 in HGrC1 cells. *Endocrinology*. 2018;**159**(4):1690–1703.
53. RRID:AB_10793856, https://antibodyregistry.org/search?q=AB_10793856.
54. RRID:AB_10796098, https://antibodyregistry.org/search?q=AB_10796098.
55. Skarra DV, Arriola DJ, Benson CA, Thackray VG. Forkhead box O1 is a repressor of basal and GnRH-induced *Fshb* transcription in gonadotropes. *Mol Endocrinol*. 2013;**27**(11):1825–1839.
56. Hume MA, Barrera LA, Gisselbrecht SS, Bulyk ML. UniPROBE, update 2015: new tools and content for the online database of protein-binding microarray data on protein–DNA interactions. *Nucleic Acids Res*. 2015;**43**(Database issue):D117–D122.

57. Rauh-Hain JA, Krivak TC, Del Carmen MG, Olawaiye AB. Ovarian cancer screening and early detection in the general population. *Rev Obstet Gynecol*. 2011;**4**(1):15–21.
58. Schumer ST, Cannistra SA. Granulosa cell tumor of the ovary. *J Clin Oncol*. 2003;**21**(6):1180–1189.
59. Young RH, Dickersin GR, Scully RE. Juvenile granulosa cell tumor of the ovary. A clinicopathological analysis of 125 cases. *Am J Surg Pathol*. 1984;**8**(8):575–596.
60. Kalfa N, Philibert P, Patte C, Thibaud E, Pienkowski C, Ecochard A, Boizet-Bonhoure B, Fellous M, Sultan C. Juvenile granulosa-cell tumor: clinical and molecular expression [in French]. *Gynécol Obstét Fertil*. 2009;**37**(1):33–44.
61. Jamieson S, Butzow R, Andersson N, Alexiadis M, Unkila-Kallio L, Heikinheimo M, Fuller PJ, Anttonen M. The FOXL2 C134W mutation is characteristic of adult granulosa cell tumors of the ovary. *Mod Pathol*. 2010;**23**(11):1477–1485.
62. Colombo N, Parma G, Zanagnolo V, Insinga A. Management of ovarian stromal cell tumors. *J Clin Oncol*. 2007;**25**(20):2944–2951.
63. Kalfa N, Veitia RA, Benayoun BA, Boizet-Bonhoure B, Sultan C. The new molecular biology of granulosa cell tumors of the ovary. *Genome Med*. 2009;**1**(8):81.
64. Carter ME, Brunet A. FOXO transcription factors. *Curr Biol*. 2007;**17**(4):R113–R114.
65. Armoni M, Harel C, Karni S, Chen H, Bar-Yoseph F, Ver MR, Quon MJ, Karnieli E. FOXO1 represses peroxisome proliferator-activated receptor-γ1 and -γ2 gene promoters in primary adipocytes. A novel paradigm to increase insulin sensitivity. *J Biol Chem*. 2006;**281**(29):19881–19891.
66. Hedrick SM. The cunning little vixen: Foxo and the cycle of life and death. *Nat Immunol*. 2009;**10**(10): 1057–1063.
67. Shaw RJ, Cantley LC. Ras, PI(3)K and mTOR signalling controls tumour cell growth. *Nature*. 2006; **441**(7092):424–430.
68. Reagan-Shaw S, Ahmad N. RNA interference-mediated depletion of phosphoinositide 3-kinase activates forkhead box class O transcription factors and induces cell cycle arrest and apoptosis in breast carcinoma cells. *Cancer Res*. 2006;**66**(2):1062–1069.
69. Massagué J, Seoane J, Wotton D. Smad transcription factors. *Genes Dev*. 2005;**19**(23):2783–2810.
70. Xu M, Chen X, Chen D, Yu B, Huang Z. FoxO1: a novel insight into its molecular mechanisms in the regulation of skeletal muscle differentiation and fiber type specification. *Oncotarget*. 2017;**8**(6): 10662–10674.
71. Yadav H, Devalaraja S, Chung ST, Rane SG. TGF-β1/Smad3 pathway targets PP2A-AMPK-FoxO1 signaling to regulate hepatic gluconeogenesis. *J Biol Chem*. 2017;**292**(8):3420–3432.
72. Palazuelos J, Klingener M, Aguirre A. TGFβ signaling regulates the timing of CNS myelination by modulating oligodendrocyte progenitor cell cycle exit through SMAD3/4/FoxO1/Sp1. *J Neurosci*. 2014; **34**(23):7917–7930.
73. Seoane J, Le HV, Shen L, Anderson SA, Massagué J. Integration of Smad and forkhead pathways in the control of neuroepithelial and glioblastoma cell proliferation. *Cell*. 2004;**117**(2):211–223.
74. Park Y, Maizels ET, Feiger ZJ, Alam H, Peters CA, Woodruff TK, Unterman TG, Lee EJ, Jameson JL, Hunzicker-Dunn M. Induction of cyclin D2 in rat granulosa cells requires FSH-dependent relief from FOXO1 repression coupled with positive signals from Smad. *J Biol Chem*. 2005;**280**(10):9135–9148.
75. Dobierzewska A, Shi L, Karakashian AA, Nikolova-Karakashian MN. Interleukin 1β regulation of FoxO1 protein content and localization: evidence for a novel ceramide-dependent mechanism. *J Biol Chem*. 2012;**287**(53):44749–44760.
76. Benayoun BA, Caburet S, Dipietromaria A, Georges A, D'Haene B, Pandaranayaka PJ, L'Hôte D, Todeschini AL, Krishnaswamy S, Fellous M, De Baere E, Veitia RA. Functional exploration of the adult ovarian granulosa cell tumor-associated somatic *FOXL2* mutation p.Cys134Trp (c.402C>G). *PLoS One*. 2010;**5**(1):e8789.
77. Nakao A, Imamura T, Souchelnytskyi S, Kawabata M, Ishisaki A, Oeda E, Tamaki K, Hanai J, Heldin CH, Miyazono K, ten Dijke P. TGF-β receptor-mediated signalling through Smad2, Smad3 and Smad4. *EMBO J*. 1997;**16**(17):5353–5362.
78. Vogt PK, Jiang H, Aoki M. Triple layer control: phosphorylation, acetylation and ubiquitination of FOXO proteins. *Cell Cycle*. 2005;**4**(7):908–913.